



Research paper

Synthesis of highly branched oligoethylenes by air-stable N,N-indazole derivate methallyl Ni(II) complexes

Claudia Araya^a, Iván Martínez-díaz^b, Sebastián A. Correa^{a,b}, Constantin G. Daniliuc^c, René S. Rojas^{a,*}

^a Departamento de Química Inorgánica, Facultad de Química y de Farmacia, Pontificia Universidad Católica de Chile, Vicuña Mackenna 4860, Macul, Santiago, Chile

^b Departamento de Ciencias Químicas y Biológicas, Universidad Bernardo O'Higgins, General Gana 1702, Santiago, Chile

^c Organisch-Chemisches Institut, Westfälische Wilhelm-Universität, Corrensstrasse 40, 48149 Münster, Germany



ARTICLE INFO

Keywords:
Ni complexes
Air-stable
Remote activation
Hyperbranched structure

ABSTRACT

Two new neutral N,N-indazole ligands bearing the carbonitrile functional group (**L1** and **L2**) and two new air-stable cationic nickel methallyl complexes (**C1** and **C2**) were prepared. These compounds were fully characterized by NMR, FT-IR and elemental analysis. In addition, compounds **L1**, **L2** and **C2** were analyzed using X-ray diffraction. The reactivity of complexes **C1** and **C2** toward ethylene was studied by using 5 equivalents of B(C₆F₅)₃. At 12.5 bar of ethylene and 20 °C, complexes **C1** and **C2** could produce oligoethylenes with a moderate activity ~ 700 kg of PE (mol of Ni)⁻¹h⁻¹. By increasing the temperature to 60 °C, the catalytic activity increased to ~ 10³ kg of PE (mol of Ni)⁻¹h⁻¹, and oligoethylenes were produced. The microstructure studied by ¹³C NMR revealed a broad distribution of branches, including methyl, ethyl, propyl, butyl and long branches. Remarkably, complexes **C1** and **C2** showed the presence *sec*-butyl branches, which are characteristic of hyperbranched microstructures. The GPC analysis result is consistent with the use of low-molecular-weight materials, and the PD1 was ~ 1, which may indicate the presence of living behavior.

1. Introduction

In 1995, a real breakthrough in the development of late transition metal catalysts to efficiently polymerize ethylene was introduced by Brookhart and coworkers [1]. Since then, a wide variety of nickel-based initiators has been studied for the polymerization of high-molecular-weight-polyethylene [2–5]. A key feature of nickel-based catalysts is their ability to polymerize ethylene *via* the “chain-walking mechanism”, which enables the production of attractive branched polymeric materials [6–8]. High-molecular-weight materials are interesting due to their mechanical and rheological properties, and active academic and industrial studies have focused on these materials. However, this concept has been shifted to another class of undeveloped materials: low-M_n highly branched polyethylenes (HBPE), which can be used as synthetic lubricants, interface active agents or viscosity modifiers and functional additives [9–11].

Group IV (PAO - polyalphaolefins) accounts for the largest product segment of the global synthetic lubricant market, and production is expected to reach US 33.8 Bn by 2023 [12]. The large global demand makes active research of the development of new catalysts that can produce HBPE materials necessary. Their synthesis can be achieved by

group-IV tandem polymerization processes [13] and tandem catalyst systems based on late transition metals [14,15]. A Pd-based catalyst can undergo extensive “chain-walking” during polymerization and produce HBPE materials [4,10]. However, they are self-limited due to their low activity. Meanwhile, nickel-based catalysts are more attractive in terms of abundant availability of the metal. Among all well-known nickel catalysts, Ni-methallyl complexes with different coordination modes, i.e., P,O; N,O or N,N (Chart 1), have been studied. Bazan et al. reported the initiator (Chart 1a), which could produce almost exclusively 1-butene [16]. Lee et al. replaced the diphenylphosphino group of initiator **1a** for the alkylideneamino group, and the initiator (Chart 1b) could produce polyethylene [17]. These examples show the ligand-induced changes in the polymerization processes. Particularly, for **1b**, the chain transfer reaction is dramatically reduced, which favors the polymer growth.

In this context, our research group has focused on the synthesis of N,N nickel complexes. Trofymchuck et al. synthesized β-diketoenamine nickel complexes (Chart 1c) that were active toward ethylene polymerization, and they obtained high-molecular-weight branched materials in good activity [18]. Cabrera et al. reported nickel complexes bearing indazole derivatives (chart 1d) that were active to ethylene

* Corresponding author.

E-mail address: rrojasg@uc.cl (R.S. Rojas).

<https://doi.org/10.1016/j.ica.2020.119761>

Received 4 April 2020; Received in revised form 11 May 2020; Accepted 11 May 2020

Available online 13 May 2020

0020-1693/ © 2020 Elsevier B.V. All rights reserved.

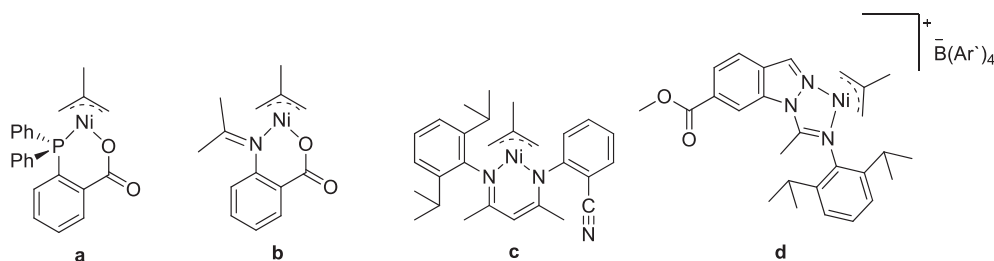


Chart 1. Selected Ni-methallyl complexes.

polymerization [19]. Interestingly, the branching pattern shows the presence of almost exclusively methyl branches; such branching control mediated by a catalyst is interesting and opens the opportunity to develop a new *N,N*-indazole ligand, which enables us to produce nickel catalysts that can control the branching content and access novel branching architectures.

Here, we report the synthesis and structural characterization of new indazole derivatives with the carbonitrile functional group in the ligand backbone. This functional group enables the remote activation of the metal center by Lewis acid as tris(pentafluorophenyl)borane, $B(C_6F_5)_3$. Upon polymerization reactions, hyperbranched low-molecular-weight materials were obtained due to the presence of *sec*-butyl branches, which are indicative of a branch-on-branch motif. This unique branching motif has not been reported in nickel methallyl complexes.

2. Experimental

2.1. General remarks

All manipulations were performed in an inert atmosphere using the standard glovebox and Schlenk-line techniques. All reagents were used as received from Aldrich unless otherwise specified. Ethylene was purchased from Matheson Tri-Gas (research grade, 99.99% pure). Toluene, THF, hexane, and pentane were distilled from benzophenone ketyl, and NEt_3 was dried over KOH. The starting compound *N*-(2-cyanophenyl)benzimidoyl [20] and $[(\eta^3-CH_3C(CH_2)_2)NiCl]_2$ [21] were synthesized according to the literature procedures. The NMR spectra were obtained using Bruker Avance 400 spectrometers. The chemical shifts are given in parts per million relative to TMS (1H and ^{13}C , $\delta(SiMe_4)$ 0) or an external standard ($\delta(BF_3 \cdot OEt_2)$ 0 for ^{11}B , $\delta(C_6H_5CF_3)$ 0, and for ^{19}F NMR). Most NMR assignments were supported by additional 2D experiments. FT-IR spectra were acquired on a Shimadzu IRTracer-100 spectrophotometer using KBr pellets. An elemental analysis (C,H,N) was performed on an Elementar Vario EL III Analyzer. X-ray diffraction was used to analyze the crystal structures. The data were collected with a Bruker D8 Venture CMOS or a Bruker APEX II CCD diffractometer and provided by Dr. Constantin G. Daniliuc; complete crystallographic details can be found in the independently recorded crystallographic information files. All polymerization reactions were performed in a Parr autoclave reactor as described below. The polymers (waxes) were dried overnight in vacuum, and the polymerization activities were calculated from the mass of the obtained product. The polymers were characterized by GPC analysis at 135 °C in *o*-dichlorobenzene (in a Polymer Laboratories, high-temperature chromatograph, PI-GPC 200). The 1H NMR spectra of the polymers were obtained in solution (C_6D_6).

2.2. Synthesis of ligands

2.2.1. Synthesis of 2-[imino(phenyl)methyl]aniline (1a)

To a cooled solution of 2-aminobenzonitrile solution in THF (1.22 g, 0.01 mol), phenylmagnesium bromide (11 mL, 0.03 mol, 3 M) was added dropwise. Then, the reaction mixture was stirred for 3 h at -10 °C. To remove the unreacted Grignard reagent, the mixture was

poured into a brine solution and extracted with diethyl ether. The organic layer was dried over Na_2SO_4 , and the solvent was removed in vacuum to afford a brown oil, which corresponded to **1a** in a 67% yield. 1H NMR (400 MHz, $CDCl_3$, 300 K): $\delta/ppm = 9.59$ (s, 1H), 7.42 (d, $J = 2.9$ Hz, 5H), 7.18 (t, $J = 7.3$ Hz, 1H), 7.07 (d, $J = 7.8$ Hz, 1H), 6.74 (d, $J = 8.0$ Hz, 1H), 6.53 (dd, $J = 22.7$, 16.3 Hz, 2H). ^{13}C NMR (101 MHz, $CDCl_3$, 300 K): $\delta/ppm = 180.29$, 133.24, 131.43, 129.25, 128.79, 128.46, 127.32, 127.20, 116.95, 116.87, 115.76.

2.2.2. Synthesis of 3-phenyl-1H-indazole (1b)

1a was added to a solution of $Cu(OAc)_2$ (0.38 g, 2.09 mmol) in DMSO. The mixture was heated at 85 °C for 3 h, subsequently poured into brine and extracted with EtOAc. The solvent was concentrated in vacuum. After purification by column chromatography (*n*-hexane/EtOAc 20:1), a yellow solid was obtained in 47.5% yield. 1H NMR (400 MHz, $CDCl_3$, 300 K): $\delta/ppm = 12.06$ (s, 1H), 8.05 (t, $J = 7.4$ Hz, 3H), 7.57 (t, $J = 7.2$ Hz, 2H), 7.48 (t, $J = 7.1$ Hz, 1H), 7.34 (t, $J = 7.5$ Hz, 1H), 7.25 – 7.15 (m, 2H). ^{13}C NMR (101 MHz, $CDCl_3$, 300 K): $\delta/ppm = 145.71$, 141.75, 133.63, 129.01, 128.24, 127.86, 126.79, 121.34, 121.06, 120.98, 110.41. Anal. Calc. for $C_{13}H_{10}N_2$: C, 80.39; H, 5.19; N, 14.42. Found: C, 80.38; H, 5.20; N, 14.40.

2.2.3. Synthesis 1-((N-(2-cyanophenyl)-1-phenylimine)indazole (L1)

N-(2-cyanophenyl)benzimidoyl chloride (0.500 g, 2.08 mmol) was added dropwise to a solution of 1H-indazole (0.250 mg, 2.08 mmol) in anhydrous toluene using triethylamine as the catalyst. The mixture was refluxed for 36 h with vigorous stirring. The yellow solution was refluxed to dryness. The crude was purified via silica gel chromatography (4:1 hexane/ethyl acetate), and **L1** was collected as a pale yellow solid in 60% yield. 1H NMR (400 MHz, $CDCl_3$, 298 K): $\delta/ppm = 8.98$ (s, 1H), 7.68 (d, $J = 8.9$ Hz, 2H), 7.53 (d, $J = 9.0$ Hz, 1H), 7.38 (m, 6H), 7.27 (m, 1H), 7.09 (m, 2H), 6.84 (d, $J = 8.0$ Hz, 1H). ^{13}C NMR (101 MHz, $CDCl_3$, 298 K): $\delta/ppm = 150.92$, 133.32, 133.01, 131.02, 130.31, 129.79, 128.62, 128.54, 128.34, 124.26, 124.01, 123.67, 122.39, 121.83, 121.24, 119.11, 117.24, 105.16. FT-IR (KBr): $\nu/cm^{-1} = 2223$ ($C\equiv N$). Anal. Calc. for $C_{21}H_{14}N_4$: C, 78.24; H, 4.38; N, 17.38. Found: C, 78.28; H, 4.32; N, 17.42.

2.2.4. Synthesis of 3-phenyl-1-((N-(2-cyanophenyl)-1-phenylimine)indazole (L2)

To a solution of 3-phenyl-1H-indazole (0.12 g, 0.63 mmol) in dry toluene, *N*-(2-cyanophenyl)benzimidoyl chloride (0.15 g, 0.63 mmol) was added. The mixture was refluxed at 80 °C for 24 h. **L2** was obtained as analytically pure yellow crystals after the column chromatography purification (ethyl acetate/hexanes 98/2) in a 68.8% yield. 1H NMR (400 MHz, $CDCl_3$, 300 K): $\delta/ppm = 8.82$ (d, $J = 8.0$ Hz, 1H), 8.07 (d, $J = 7.9$ Hz, 1H), 7.88 (d, $J = 6.4$ Hz, 2H), 7.63 (t, $J = 7.0$ Hz, 1H), 7.53 (d, $J = 7.7$ Hz, 1H), 7.50 – 7.40 (m, 6H), 7.40–7.30 (m, 4H), 7.02 (t, $J = 7.5$ Hz, 1H), 6.82 (d, $J = 7.9$ Hz, 1H). ^{13}C NMR (101 MHz, $CDCl_3$, 300 K): $\delta/ppm = 157.80$, 152.08, 148.87, 141.32, 132.99, 132.80, 132.23, 131.50, 130.15, 129.88, 129.08, 128.80, 128.14, 127.83, 124.90, 124.53, 123.21, 122.36, 121.23, 117.81, 116.78, 105.60. FT-IR (KBr): $\nu/cm^{-1} = 2217$ ($C\equiv N$). Anal. Calc. for $C_{27}H_{18}N_4$: C, 81.39; H, 4.55; N, 14.06. Found: C, 81.38; H, 4.55; N, 14.07.

2.3. Synthesis of complexes

2.3.1. Synthesis of (1-((N-(2-cyanophenyl)-1-phenylimino)indazole)(η^3 -methylallyl)nickel(II) tetrafluoroborate (C1)

L1 (645 mg, 2.0 mmol) and NaBF_4 (109 mg, 0.99 mmol) were mixed in dichloromethane (10 mL). The suspension was vigorously stirred, and a solution of $[(\eta^3\text{-CH}_3\text{C}(\text{CH}_2)_2\text{NiCl})_2]$ (300 mg, 0.99 mmol) in dichloromethane was added. The mixture was stirred for 2 h at room temperature. The resulting solution was filtered through celite, and a red crystalline solid was obtained by adding pentane and storing at -30°C in 75% yield. ^1H NMR (400 MHz, CDCl_3 , 298 K): δ/ppm = 8.17 (s, 1H), 7.63 (m, 2H), 7.59 (m, 1H), 7.41 (m, 6H), 7.33 (m, 2H), 7.08 (m, 1H), 3.46 (s, 1H), 3.18 (s, 1H), 2.72 (s, 1H), 2.65 (s, 1H), 2.28 (s, 3H). ^{13}C NMR (400 MHz, CDCl_3 , 298 K): δ/ppm = 163.6, 152.5, 148.5, 136.1, 134.7, 134.1, 133.5, 131.7, 129.8, 128.5, 127.0, 123.5, 123.4, 122.6, 115.7, 106.9, 60.1, 23.3. ^{19}F NMR (400 MHz, CDCl_3 , 298 K): δ/ppm = m, -157.22 . ^{11}B NMR (400 MHz, CDCl_3 , 298 K): δ/ppm = s, -1.23 . FT-IR (KBr): ν/cm^{-1} = 2221 (C \equiv N). Anal. Calc. for $\text{C}_{25}\text{H}_{24}\text{BF}_4\text{N}_4\text{Ni}$: C, 57.09; H, 4.60; N, 10.65. Found: C, 56.92; H, 4.55; N, 11.07.

2.3.2. Synthesis of (3-phenyl-1((N-(2-cyanophenyl)-1-phenylimino)indazole)(η^3 -methylallyl)nickel(II) tetrafluoroborate (C2)

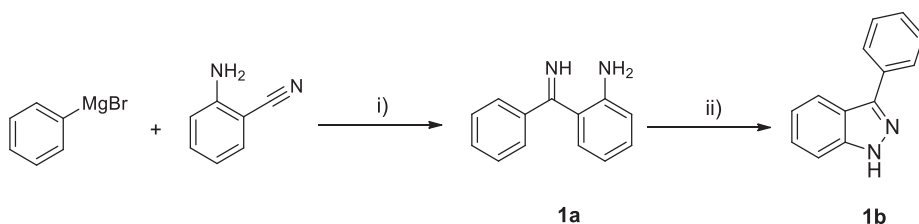
L2 (797 mg, 2.0 mmol) and NaBF_4 (109 mg, 0.99 mmol) were mixed in dichloromethane (10 mL). The suspension was vigorously stirred, and a solution of $[(\eta^3\text{-CH}_3\text{C}(\text{CH}_2)_2\text{NiCl})_2]$ (300 mg, 0.99 mmol) in dichloromethane was added. The mixture was stirred for 2 h at room temperature. The resulting solution was filtered through celite and dried in vacuum. The solid was washed with cooled dichloromethane, and recrystallization occurred in pentane at -30°C overnight, which yielded a brown solid in 76%. ^1H NMR (400 MHz, CDCl_3 , 300 K): δ/ppm = 7.98 (d, J = 7.2 Hz), 7.85 (d, J = 7.1 Hz), 7.69 – 7.58 (m, 4H), 7.58 – 7.49 (m, 4H), 7.49 – 7.41 (m, 2H), 7.34 – 7.27 (m, 2H), 7.18 (t, J = 7.7 Hz, 1H), 5.87 (d, J = 7.9 Hz, 1H), 2.50 (s, 1H), 2.43 (s, 1H), 2.36 (s, 1H), 2.30 (s, 1H), 2.12 (s, 3H). ^{13}C NMR (101 MHz, CDCl_3 , 300 K): δ/ppm = 161.75, 158.63, 149.93, 139.22, 134.65, 132.36, 132.10, 132.01, 131.19, 130.23, 130.05, 129.20, 128.89, 127.08, 126.88, 126.77, 126.49, 126.03, 125.86, 123.53, 112.22, 107.16, 58.24, 57.64, 53.59, 53.26, 22.88. FT-IR (KBr): ν/cm^{-1} = 2225 (C \equiv N). Anal. Calc. for $\text{C}_{31}\text{H}_{28}\text{BF}_4\text{N}_4\text{Ni}$: C, 61.84; H, 4.69; N, 9.31. Found: C, 61.38; H, 4.55; N, 9.87.

3. Results and discussion

3.1. Synthesis and characterization of cationic methallyl Ni complexes

Scheme 1 shows the reaction pathway of the formation of the 3-substituted 1H-indazole. The reaction proceeds via the nucleophilic attack of phenylmagnesium bromide of the nitrile functional group of *o*-aminobenzonitrile. The resulting *o*-aminoaryl N–H ketimine (**1a**) can react with a catalytic amount of $\text{Cu}(\text{OAc})_2$, which facilitated N–N bond formation to yield the desired 3-phenyl-1H-indazole (**1b**) [22].

Scheme 2 shows the reaction path to ligands **L1** and **L2**. The ligands were synthesized by the reaction of *N*-(2-cyanophenyl)benzomidoil chloride with 1H-indazole and 3-phenyl-1H-indazole in the presence of Et_3N in toluene at reflux. Each ligand was isolated as a pale-yellow solid



Scheme 1. Synthesis of 3-phenyl-1H-indazole. i) THF, ii) $\text{Cu}(\text{OAc})_2$, DMSO.

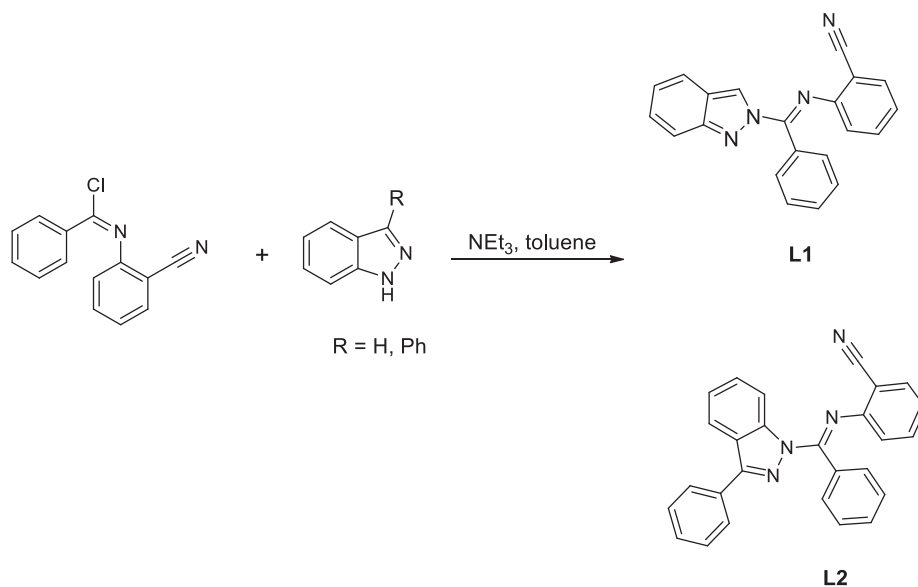
in a good yield, and they were fully characterized by NMR spectroscopy, FT-IR, elemental analysis and X-ray crystallography.

The elemental analysis is consistent with the ligands in **Scheme 2**. However, the regiochemistry can be modulated by the reaction conditions to obtain one of the N-1 or N-2 substituted indazole regioisomers. We use a nondeprotonating base as NEt_3 , which is a well-known N-2 directed [23]. ^1H , ^{13}C NMR and FT-IR analysis are consistent with the formation of a single isomer for compounds **L1** and **L2**. For example, only one peak for the nitrile ^{13}C NMR chemical shift was observed for each ligand at ~ 117.8 ppm, and a stretching band appears at 2221 and 2225 cm^{-1} in the FT-IR. However, these results cannot help us distinguish the two regioisomers.

An X-ray diffraction study was performed to identify the chemical structure for both ligands; single crystals for **L1** and **L2** were grown in ether/*n*-hexane (1:3). **Fig. 1** shows the structure for both ligands. As expected, an N-2 substituted indazole was obtained for **L1** due to the use of Et_3N as a nondeprotonating base. However, **L2** shows a N-1 substituted indazole probably due to the steric hindrance around the 3-phenyl moiety, which makes the N-1 attack more prone to nucleophilic attack. These ligands exhibit an E configuration in the imine; meanwhile, the nitrile group is in plane for **L1**, and the **L2** nitrile group is orthogonal to the indazole plane. For further details of the X-ray characterization, see **Supplementary data**.

The methallyl nickel complexes were prepared by adding two equivalent of the respective ligand with one equivalent of $[(\eta^3\text{-CH}_3\text{C}(\text{CH}_2)_2\text{NiCl})_2]$ in the presence of one equivalent of NaBF_4 . The target complexes **C1** and **C2** are red and brown solids in 75 and 76% yields, respectively (**Scheme 3**). ^1H and ^{13}C NMR spectra in CDCl_3 for both complexes are consistent with the formation of a single isomer containing a nickel center ligated in an N,N fashion and $\eta^3\text{-(CH}_2)_2\text{Me}$. Complex **C1** features four separate resonances for the *syn* and *anti* allylic hydrogen atoms at δ 2.65, 2.72 (H_{syn}) and 3.18, 3.40 (H_{anti}) ppm. Meanwhile, complex **C2** shows *syn* and *anti* allylic hydrogen atoms at δ 2.30, 2.36 (H_{syn}) and 2.43, 2.50 (H_{anti}) ppm. The resonances of *anti* allylic hydrogen atoms appeared as broadened signals compared to the *syn* allylic hydrogen atoms, which suggests a fluxional behavior of the allyl moiety on the NMR time scale. [24,25] BF_4^- counter ion NMR singlets in CDCl_3 are consistent with “free” ions and are not an ion-pairing with the cationic complex parts. (^{11}B : -0.68 ppm, $\nu_{1/2}$ = 11 Hz; ^{19}F : -151.77 ppm) [19].

The molecular structure for **C2** was determined by an X-ray diffraction study and is shown in **Fig. 2**. The crystal structure of the complex confirms a four-coordinated nickel metal center, which adopts an almost ideal square-planar geometry. The methallyl group was found disordered over two positions with a ratio of 81:19. Only the main disordered part of this methallyl group is discussed below. The dihedral angle corresponding to the N,N chelate section is -2.6° (N1-C41-C43-N3). The N3-Ni1-N1, N3-Ni1-C43 N1-Ni1-C41 and C43-Ni1-C41 angles were $82.9(1)$, $101.4(2)$, $104.3(2)$ and $71.5(2)^\circ$, respectively. The Ni1-N1, Ni1-N3, Ni1-C42, Ni1-N43 and Ni1-C41 bond distances were $1.924(3)$, $1.923(3)$, $1.982(5)$, $2.011(5)$ and $2.020(4)$ Å, respectively. The C37-N4 bond distance of $1.144(7)$ indicate the presence of a triple bond [18,26,27]. Additionally, the cyanophenyl substituent is orthogonal to the indazole plane (dihedral angle: $80.5(8)^\circ$ (C8-N3-C31-C36)), and the CN functionality is free to coordinate the Lewis acid. Additional X-ray details have been reported in the **Supplementary data**.



Scheme 2. Synthetic route for ligands L1 and L2.

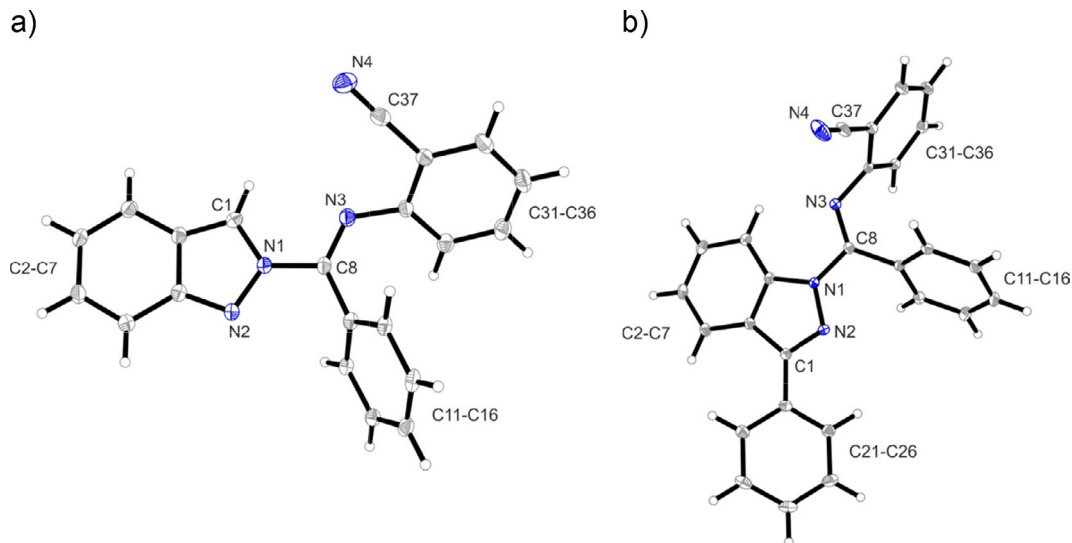
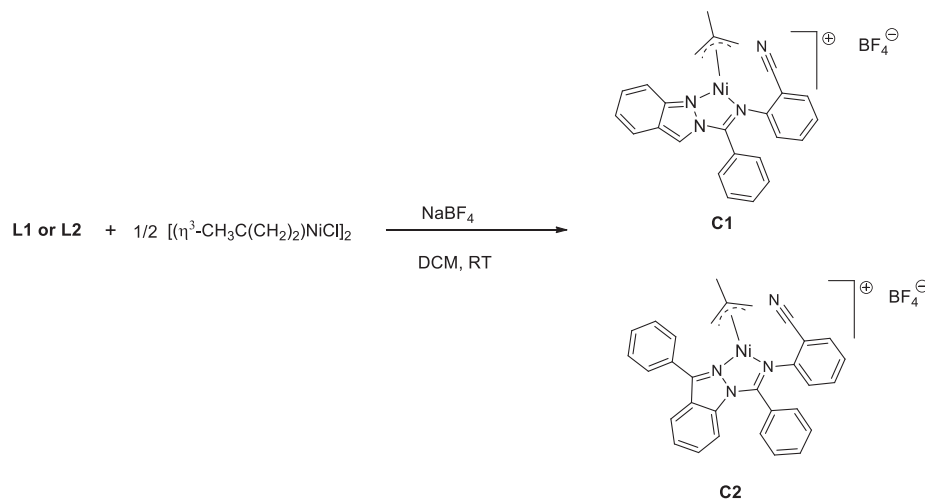


Fig. 1. a) X-ray crystal structure of ligands L1 and b) L2. The thermal ellipsoids are set at 30% probability.



Scheme 3. Synthetic route for complexes C1 and C2.

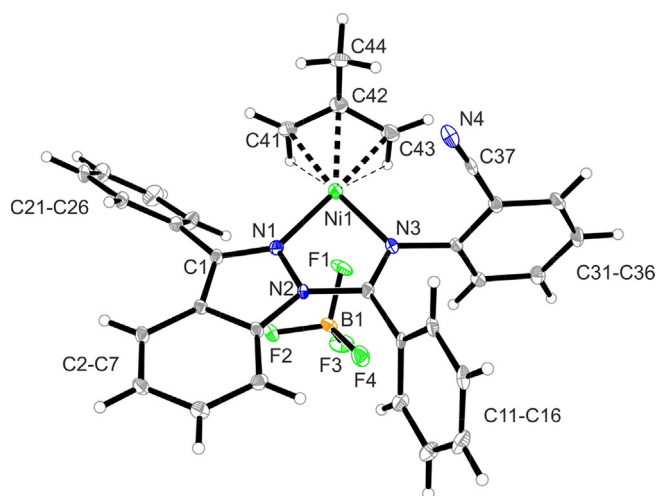


Fig. 2. X-ray crystal structure of **C2** with thermal ellipsoids at the 30% probability. Only the main disordered parts of methallyl and 2-cyanophenyl groups are shown.

3.2. Reactivity of complexes toward ethylene

Methallyl nickel complexes require a coactivator to generate the active species. For this purpose, we select tris(pentafluorophenyl) borane ($B(C_6F_5)_3$) because it easily coordinates with the carbonitrile functional group [5,18,19,23–25]. Complexes **C1** and **C2** were reacted with 1 equivalent of ($B(C_6F_5)_3$) in $CDCl_3$ solution at room temperature. The NMR characterization by ^{11}B and ^{19}F is characteristic for the Lewis acid adduct formation (*in situ*). In the ^{19}F NMR spectrum, three signals at -134.6, -156.2 and -163.6 ppm indicate the attachment of the ($B(C_6F_5)_3$) Lewis acid. The separation of the resonances of the *meta* and *para* fluorine substituents by $\Delta m,p = 7.4$ ppm indicates the presence of a distinctly changed tetracoordinated boron compared to tricoordinated ($B(C_6F_5)_3$), $\Delta m,p = 20.1$ ppm, but it is similar to that of the pyridine adduct (C_6F_5) $_3$ $B-NC_5H_5$ with $\Delta m,p = 7.2$ ppm [29]. The ^{11}B NMR resonance at -10.2 ppm also confirms a tetracoordinated boron [28,30].

A series of reference experiment showed that **C1** and **C2** that were activated with one equivalent of ($B(C_6F_5)_3$) were not active toward ethylene (entry 1, Table 1). This result was expected due to the slow initiation rates in methallyl nickel complexes, even when they were activated with a strong Lewis acid as ($B(C_6F_5)_3$) [24,31]. Another fact to consider is that this adduct is “labile”, which implies that there is the dissociation of nitrile from borane, followed by recoordination [18,26]. Thus, the complex reactivity was tested with five equivalents of ($B(C_6F_5)_3$) as the coactivator at 12.5 bar and 20 and 60 °C (Table 1).

As expected, under these conditions, the kinetics ethylene oligomerization is accelerated for complexes **C1** and **C2**. These enhanced activities are possible through the acid-base Lewis interaction between boron atom and cyano group in the ligand backbone, which is

Table 1
Selected oligomerization reactions.

Entry*	Complex	T (°C)	activity ^a	Mw ^b	Mn ^b	PDI ^c
1	C1, C2	20, 60	0	–	–	–
2	C1	20	690	906	856	1.05
3	C2	20	711	757	743	1.01
4	C1	60	1.102	915	857	1.07
5	C2	60	1.234	1011	928	1.08

^a Activity is presented in units of kg of PE (mol of Ni) $^{-1}h^{-1}$. ^b Molecular weights are presented in units of g mol $^{-1}$. Molecular weights were determined by GPC. ^c Polydispersity index. * Entry 1, complexes **C1** and **C2** were activated with one equivalent of ($B(C_6F_5)_3$). Entries 2–5, complexes **C1** and **C2** were activated with five equivalents of ($B(C_6F_5)_3$).

conjugated with the nickel center. This interaction removes electron density from the nickel core and makes it more prone to ethylene coordination. Despite the cationic nature of these complexes, they proved to be air-stable, which shows the same NMR pattern and ethylene oligomerization activity after being exposed to ambient atmosphere for 48h and 7 days.

3.3. Oligomer characterization

Viscous materials were recovered from the reactor. The microstructural analysis of oligoethylenes by ^{13}C NMR showed the presence of methyl, ethyl, propyl, butyl, *sec*-butyl and long branches for all samples (Table 2). Interestingly, *sec*-butyl moieties were found (Fig. 3), which indicates that the microstructure is hyperbranched, since the presence of *sec*-butyl is indicative of branch-on-branch moieties. It is well-known that the branching densities and microstructure of oligo/polyethylenes are greatly affected by the behavior of Ni or Pd agostic alkyl intermediates [32,33]. These species can undergo “chain-walking” via β -hydride elimination, olefin rotation and reinsertion. NMR studies have shown that the barrier to a 1,2 shift in Ni agostic intermediates is ca. 14 Kcal/mol, while for Pd agostic intermediates, the 1,2-*chain-walking* is lower (9–10 kcal/mol), which implies that many 1,2-shifts occur prior to insertion and yield hyperbranched structures [34]. To the best of our knowledge, such microstructure has not been reported in other methallyl nickel complexes reported in the literature.

The presence of phenyl ring in the **C1** (Fig. 2) indazole framework does not have a large effect on the activity and microstructure pattern; this relative insensibility is due to its poor steric hindrance around the nickel center. Finally, the GPC analysis reveals a low-molecular-weight oligomer with a polydispersity index ~ 1 , which suggests that this catalyst may exhibit a living behavior [35,36].

4. Conclusion

In summary, we prepared two new *N,N*-indazole ligands (**L1** and **L2**), which were characterized by NMR spectroscopy, FT-IR, elemental analysis and X-ray diffraction [37]. In addition, two new organometallic species were isolated and characterized: The complexes **C1** and **C2**. Complex **C2** was fully characterized by 1H , ^{13}C , ^{11}B and ^{19}F NMR, FT-IR, elemental analysis and X-ray diffraction [37].

A series of oligomerization reactions was performed, which shows that complexes **C1** and **C2** produced hyperbranched low-molecular-weight oligoethylenes. Interestingly, the microstructure pattern studied by ^{13}C NMR spectroscopy revealed the presence of *sec*-butyl moieties, which have not been found in nickel methallyl complexes. Thus, the design of new *N,N*-indazole derivatives will allow one to obtain a new catalyst that can generate oli/polyethylenes with interesting microstructures.

The GPC analysis reveals that these systems can behave as living oligomerization catalysts. Future work will be directed to the study of the living behavior and theoretical properties of the oligomerization mechanism.

5. Author statement

These authors contributed equally.

Declaration of Competing Interest

The authors declare that they have no known competing financial interests or personal relationships that could have appeared to influence the work reported in this paper.

Table 2
Microstructure distribution.

Entry	Complex	Branches/1000C ^a	Methyl ^b	Ethyl ^b	Propyl ^c	Butyl ^d	Sec-butyl ^e	Long ^f
1	C1, C2	–	–	–	–	–	–	–
2	C1	74	57	7	4	6	7	19
3	C2	89	47	9	7	11	9	17
4	C1	70	55	7	5	6	7	20
5	C2	87	45	9	8	10	8	20

^a The degree of branching was calculated from the ¹H NMR intensity ratios of the methyl groups (and corrected for the saturated end groups vs. the overall integral).

^b Percentages of different branch lengths can be calculated from the relative intensity ratios of the methyl (1B₁, 1B₂) or methine (C₄₊) signals of the respective branches in the ¹³C NMR spectra.

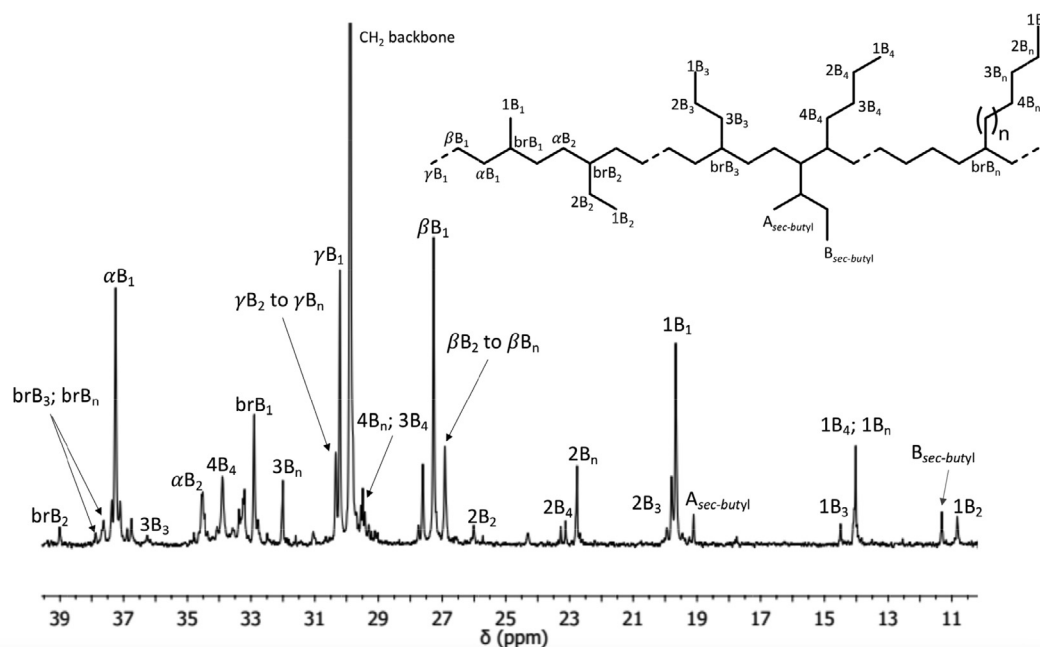


Fig. 3. ¹³C NMR spectrum of hyperbranched polyethylene obtained with C1. (Table 1, entry 2).

Acknowledgment

This work was supported by FONDECYT project no. 1161091, CONICYT (grant. No. 21140118) and FONDECYT (postdoctoral fellowship 3160480) of Chile.

Appendix A. Supplementary data

Supplementary data to this article can be found online at <https://doi.org/10.1016/j.ica.2020.119761>.

References

- L.K. Johnson, C.M. Killian, M. Brookhart, New Pd(II)- and Ni(II)-Based Catalysts for Polymerization of Ethylene and α -Olefins, *J. Am. Chem. Soc.* 117 (1995) 6414–6415. <https://doi.org/10.1021/ja00128a054>.
- H. Mu, L. Pan, D. Song, Y. Li, Neutral Nickel Catalysts for Olefin Homo- and Copolymerization: Relationships between Catalyst Structures and Catalytic Properties, *Chem. Rev.* 115 (2015) 12091–12137. <https://doi.org/10.1021/cr500370f>.
- S. Wang, W.-H. Sun, C. Redshaw, Recent progress on nickel-based systems for ethylene oligo-/polymerization catalysis, *J. Organomet. Chem.* 751 (2014) 717–741. <https://doi.org/10.1016/j.jorganchem.2013.08.021>.
- J. Wang, L. Wang, H. Yu, R.S. Ullah, M. Haroon, X. Zain-ul-Abdin, R.U. Khan Xia, Recent Progress in Ethylene Polymerization Catalyzed by Ni and Pd Catalysts, *Eur. J. Inorg. Chem.* 2018 (2018) 1450–1468. <https://doi.org/10.1002/ejic.201701336>.
- B.M. Boardman, G.C. Bazan, α -Iminocarboxamidato Nickel Complexes, *Acc. Chem. Res.* 42 (2009) 1597–1606. <https://doi.org/10.1021/ar900097b>.
- L. Guo, S. Dai, X. Sui, C. Chen, Palladium and Nickel Catalyzed Chain Walking Olefin Polymerization and Copolymerization, *ACS Catal.* 6 (2016) 428–441. <https://doi.org/10.1021/acscatal.5b02426>.
- T.R. Younkin, E.F. Connor, J.I. Henderson, S.K. Friedrich, R.H. Grubbs, D.A. Bansleben, Neutral, Single-Component Nickel (II) Polyolefin Catalysts That Tolerate Heteroatoms, *Science* 287 (2000) 460–462. <https://doi.org/10.1126/science.287.5452.460>.
- R. Dockhorn, L. Plüschke, M. Geisler, J. Zessin, P. Lindner, R. Mundil, J. Merna, J.-U. Sommer, A. Lederer, Polyolefins Formed by Chain Walking Catalysis—A Matter of Branching Density Only? *J. Am. Chem. Soc.* 141 (2019) 15586–15596. <https://doi.org/10.1021/jacs.9b06785>.
- Z. Dong, Z. Ye, Hyperbranched polyethylenes by chain walking polymerization: synthesis, properties, functionalization, and applications, *Polym. Chem.* 3 (2012) 286–301. <https://doi.org/10.1039/C1PY00368B>.
- L. Xu, Z. Ye, A Pd–diimine catalytic inimer for synthesis of polyethylenes of hyperbranched-on-hyperbranched and star architectures, *Chem. Commun.* 49 (2013) 8800–8802. <https://doi.org/10.1039/C3CC45101A>.
- I. D'Auria, S. Milione, T. Caruso, G. Balducci, C. Pellecchia, Synthesis of hyperbranched low molecular weight polyethylene oils by an iminopyridine nickel(II) catalyst, *Polym. Chem.* 8 (2017) 6443–6454. <https://doi.org/10.1039/C7PY01215B>.
- Synthetic Lubricants Market, Size, Share And Forecasts To 2023, (n.d.). <https://www.credenceresearch.com/report/synthetic-lubricants-market>.
- M. Stürzel, S. Mihan, R. Müllhaupt, From Multisite Polymerization Catalysis to Sustainable Materials and All-Polyolefin Composites, *Chem. Rev.* 116 (2016) 1398–1433. <https://doi.org/10.1021/acs.chemrev.5b00310>.
- R.W. Barnhart, G.C. Bazan, T. Mourey, Synthesis of Branched Polyolefins Using a Combination of Homogeneous Metallocene Mimics, *J. Am. Chem. Soc.* 120 (1998) 1082–1083. <https://doi.org/10.1021/ja9735867>.
- Y. Gao, J. Chen, Y. Wang, D.B. Pickens, A. Motta, Q.J. Wang, Y.-W. Chung, T.L. Lohr, T.J. Marks, Highly branched polyethylene oligomers via group IV-catalyzed polymerization in very nonpolar media, *Nat. Catal.* 2 (2019) 236–242. <https://doi.org/10.1038/s41929-018-0224-0>.
- Z.J.A. Komon, X. Bu, G.C. Bazan, Synthesis, Characterization, and Ethylene Oligomerization Action of [(C6H5)2PC6H4C(O-B(C6F5)3)O- κ 2P, O]Ni(η -3-CH2C6H5), *J. Am. Chem. Soc.* 122 (2000) 12379–12380. <https://doi.org/10.1021/ja002042t>.
- B.Y. Lee, X. Bu, G.C. Bazan, Pyridinecarboxamidato–Nickel(II) Complexes,

- Organometallics 20 (2001) 5425–5431, <https://doi.org/10.1021/om010576c>.
- [18] O.S. Trofymchuk, D.V. Gutsulyak, C. Quintero, M. Parvez, C.G. Daniliuc, W.E. Piers, R.S. Rojas, N-Arylciano- β -diketiminate Methallyl Nickel Complexes: Synthesis, Adduct Formation, and Reactivity toward Ethylene, *Organometallics* 32 (2013) 7323–7333, <https://doi.org/10.1021/om400847b>.
- [19] A.R. Cabrera, I. Martinez, C.G. Daniliuc, G.B. Galland, C.O. Salas, R.S. Rojas, New air stable cationic methallyl Ni complexes bearing imidoyl-indazole carboxylate ligand: Synthesis, characterization and their reactivity towards ethylene, *J. Mol. Catal. A: Chem.* 414 (2016) 19–26, <https://doi.org/10.1016/j.molcata.2015.12.020>.
- [20] C. Quintero, M. Valderrama, A. Becerra, C.G. Daniliuc, R.S. Rojas, Synthesis of 4(3H)quinazolinimines by reaction of (E)-N-(aryl)-acetimidoyl or -benzimidoyl chloride with amines, *Org. Biomol. Chem.* 13 (2015) 6183–6193, <https://doi.org/10.1039/C5OB00444F>.
- [21] J. Heinicke, M. Köhler, N. Peulecke, M.K. Kindermann, W. Keim, M. Köckerling, Cationic Methallylnickel and (Meth)allylpalladium 2-Phosphinophenol Complexes: synthesis, Structural Aspects, and Use in Oligomerization of Ethylene, *Organometallics* 24 (2005) 344–352, <https://doi.org/10.1021/om049474n>.
- [22] C. Chen, G. Tang, F. He, Z. Wang, H. Jing, R. Faessler, A Synthesis of 1H-Indazoles via a Cu(OAc)₂-Catalyzed N-N Bond Formation, *Org. Lett.* 18 (2016) 1690–1693, <https://doi.org/10.1021/acs.orglett.6b00611>.
- [23] R. Caris, B.C. Peoples, M. Valderrama, G. Wu, R. Rojas, Mono and bimetallic nickel bromide complexes bearing azolate-imine ligands: Synthesis, structural characterization and ethylene polymerization studies, *J. Organomet. Chem.* 694 (2009) 1795–1801, <https://doi.org/10.1016/j.jorganchem.2009.01.005>.
- [24] M.A. Escobar, O.S. Trofymchuk, B.E. Rodríguez, C. Lopez-Lira, R. Tapia, C. Daniliuc, H. Berke, F.M. Nachtigall, L.S. Santos, R.S. Rojas, Lewis Acid Enhanced Ethene Dimerization and Alkene Isomerization—ESI-MS Identification of the Catalytically Active Pyridyldimethoxybenzimidazole Nickel(II) Hydride Species, *ACS Catal.* 5 (2015) 7338–7342, <https://doi.org/10.1021/acscatal.5b02003>.
- [25] B. Rodríguez, D. Cortés-Arriagada, E.P. Sánchez-Rodríguez, R.A. Toscano, M.C. Ortega-Alfaro, J.G. López-Cortés, A. Toro-Labbé, R.S. Rojas, B(C₆F₅)₃ Promotes the catalytic activation of [N, S]-ferrocenyl nickel complexes in ethylene oligomerization, *Appl. Catal. A* 550 (2018) 228–235, <https://doi.org/10.1016/j.apcata.2017.11.015>.
- [26] S.A. Correa, C.G. Daniliuc, H.S. Stark, R.S. Rojas, Nickel Catalysts Activated by rGO Modified with a Boron Lewis Acid To Produce rGO-Hyperbranched PE Nanocomposites, *Organometallics* 38 (2019) 3327–3337, <https://doi.org/10.1021/acs.organomet.9b00397>.
- [27] B.M. Boardman, J.M. Valderrama, F. Muñoz, G. Wu, G.C. Bazan, R. Rojas, Remote Activation of Nickel Complexes by Coordination of B(C₆F₅)₃ to an Exocyclic Carbonitrile Functionality, *Organometallics* 27 (2008) 1671–1674, <https://doi.org/10.1021/om700933y>.
- [28] A.R. Cabrera, Y. Schneider, M. Valderrama, R. Fröhlich, G. Kehr, G. Erker, R.S. Rojas, Synthesis of a [π -Cyano-nacnac]Cp]zirconium Complex and Its Remote Activation for Ethylene Polymerization, *Organometallics* 29 (2010) 6104–6110, <https://doi.org/10.1021/om100866t>.
- [29] S.L. Scott, B.C. Peoples, C. Yung, R.S. Rojas, V. Khanna, H. Sano, T. Suzuki, F. Shimizu, Highly dispersed clay–polyolefin nanocomposites free of compatibilizers, via the in situ polymerization of α -olefins by clay-supported catalysts, *Chemical Communications*. (2008) 4186, <https://doi.org/10.1039/b718241d>.
- [30] R.S. Rojas, B.C. Peoples, A.R. Cabrera, M. Valderrama, R. Fröhlich, G. Kehr, G. Erker, T. Wiegand, H. Eckert, Synthesis and Structure of Bifunctional Zirconocene/Borane Complexes and Their Activation for Ethylene Polymerization, *Organometallics* 30 (2011) 6372–6382, <https://doi.org/10.1021/om200536z>.
- [31] J.D. Azoulay, Z.A. Koretz, G. Wu, G.C. Bazan, Well-Defined Cationic Methallyl α -Keto- β -Diimine Complexes of Nickel, *Angew. Chem. Int. Ed.* 49 (2010) 7890–7894, <https://doi.org/10.1002/anie.201003125>.
- [32] H. Xu, P.B. White, C. Hu, T. Diao, Structure and Isotope Effects of the β -H Agostic (α -Diimine)Nickel Cation as a Polymerization Intermediate, *Angew. Chem. Int. Ed.* 56 (2017) 1535–1538, <https://doi.org/10.1002/anie.201611282>.
- [33] H. Xu, C.T. Hu, X. Wang, T. Diao, Structural Characterization of β -Agostic Bonds in Pd-Catalyzed Polymerization, *Organometallics* 36 (2017) 4099–4102, <https://doi.org/10.1021/acs.organomet.7b00666>.
- [34] Z. Chen, M. Brookhart, Exploring Ethylene/Polar Vinyl Monomer Copolymerizations Using Ni and Pd α -Diimine Catalysts, *Acc. Chem. Res.* 51 (2018) 1831–1839, <https://doi.org/10.1021/acs.accounts.8b00225>.
- [35] L. Zhong, G. Li, G. Liang, H. Gao, Q. Wu, Enhancing Thermal Stability and Living Fashion in α -Diimine-Nickel-Catalyzed (Co)polymerization of Ethylene and Polar Monomer by Increasing the Steric Bulk of Ligand Backbone, *Macromolecules* 50 (2017) 2675–2682, <https://doi.org/10.1021/acs.macromol.7b00121>.
- [36] K.E. Allen, J. Campos, O. Daugulis, M. Brookhart, Living Polymerization of Ethylene and Copolymerization of Ethylene/Methyl Acrylate Using “Sandwich” Diimine Palladium Catalysts, *ACS Catal.* 5 (2015) 456–464, <https://doi.org/10.1021/cs5016029>.
- [37] CCDC-1969335 (L1), -1969336 (L2), and -1969337 (C2) contain the supplementary crystallographic data for this paper. These data can be obtained free of charge from The Cambridge Crystallographic Data Centre via www.ccdc.cam.ac.uk/data_request/cif.